Hindawi
International Journal of Chemical Engineering
Volume 2022, Article ID 6748678, 12 pages
https://doi.org/10.1155/2022/6748678

Research Article

Experimental Studies of Thermal Hydraulics of Deep Eutectic Solvent Based on Choline Chloride

Myung Hyun Pyo, Siwon Seo, and Jaeyoung Lee

School of Control and Mechanical Engineering, Handong Global University, Pohang 37554, Republic of Korea

Correspondence should be addressed to Jaeyoung Lee; jylee378@gmail.com

Received 24 February 2022; Revised 7 July 2022; Accepted 3 August 2022; Published 1 September 2022

Academic Editor: Chuanxi Yang

Molten salt reactor (MSR) is considered a promising 4th generation nuclear power plant because of its safety and suitability for SMR (small modular reactor). Also, molten salts are used in concentrating solar power (CSP) and energy storage system (ESS) as a heat storage medium. So molten salt has recently been researched a lot as heat storage and a transfer medium. However, molten salts' high operating temperature (>450°C) and high Prandtl number make it hard to perform a thermal-hydraulic experiment in the laboratory. Thus, high Prandtl number and high viscosity fluid, deep eutectic solvents (DES), is chosen as a simulant of molten salts in this study. Thermal-hydraulic experiment using glyceline, which is easy to synthesize and transparent to visualize flow with high viscosity among various DESs, was performed. Also, the friction factor and heat transfer coefficient required for energy system designs were measured. As a result, it was found that glyceline is a Newtonian fluid, and the transition region from laminar to turbulent flow has a lower Reynolds number than water has. In addition, the heat transfer coefficient properties of glyceline were somewhat consistent with the existing correlations. To summarize, glyceline's friction factor and heat transfer coefficient are predictable in existing theories, but the transition regions for those are different because flow development behavior between hydraulic and thermal boundary layers is different. Therefore, it is estimated that thermal-hydraulic experiments are essential when using high Pr numbers and high viscosity fluids such as DESs and molten salts as heat storage and transfer mediums.

1. Introduction

Molten salt reactor is one of the 4th generation nuclear reactors, and it can exclude severe accidents inherently due to liquid fuel. Various molten salts used as a heat transfer medium in MSR and research on the thermophysical properties and thermal-hydraulic characteristics have been studied since 1950s. (W. B. Cottrell et al., "Reactor Program of the Aircraft Nuclear Propulsion Project," ORNL-1234 (1952)). Molten salts used as a heat storage medium in not only the nuclear field but also the renewable energy field. Concentrating solar power (CSP) is a power plant that stores solar thermal energy in a storage medium and then uses the stored heat energy to produce electricity. Usually, fluoride, chloride, and nitrate molten salts are used, and various combinations of molten salts exist. Although the melting point of molten salt is lowered by eutectic reaction, the melting temperature of the molten salts usually exceeds 400°C. It means molten salts have stability at high temperatures as a thermal storage medium. Expectations for energy storage system (ESS) applications of molten salts are also getting increased. Currently, batteries are mainly used as an ESS medium for renewable energy, but battery fire incidents have been frequently reported, and since its price is high, this causes a factor that increases the cost of ESS. And there is a limit to the capacity increase with just the batteries [1, 2]. Therefore, thermochemical heat storage and power generation system have been proposed as ESS [3]. It is possible to store a huge amount of energy in molten salts and produce electrical energy from the stored heat energy in molten salts. It is also possible to store waste heat in a molten salt storage system as well as renewable energy [4]. When electricity is required, steam may be produced from stored thermal energy, or electricity could be generated using a

supercritical carbon dioxide power generation loop. Since molten salts are being used as a heat transfer and storage medium in the fields of nuclear and renewable energy, which are carbon-free energy sources, it is very important to know the thermal-hydraulic characteristics of molten salts.

However, due to the high operating temperature and corrosive properties of molten salts, it is not easy to perform the thermal-hydraulic experimental study in the laboratory. Accordingly, studies on similar substances using thermal oil have been conducted [5], but in the case of thermal oil, the viscosity is not as high as molten salts, so it is not suitable as a simulant of molten salts. Therefore, DES (deep eutectic solvent) introduced by Abbot et al. in 2003 [6, 7] was selected in this study as an alternative material for molten salts that has high Prandtl number and high viscosity characteristics and is easy to analyze in laboratories. DES is not a type of existing IL (ionic liquid) or salt mixed with each other but a mixture of salts and organic solvents. Basically, DESs are mixtures of two or more compounds, and the mixtures have a melting point that is lower than that of the individual compounds [8]. The physicochemical properties of DESs are much like those of conventional ILs [9]. However, DESs have many advantages over conventional ILs, including the simplicity of the synthesis, lower production cost, low or negligible toxicity profiles, and sustainability with respect to environmental and economic benefits [10]. In this paper, fundamental thermal-hydraulic research of a high Prandtl number and high viscosity heat transfer fluid was conducted using glyceline, a transparent and easy to synthesize choline chloride-based DES among various DES as a simulant of molten salts.

Section 2 of this paper summarizes the characteristics of molten salts, ILs, and DESs and organizes the existing correlations for friction factor and heat transfer coefficient with high Prandtl number fluids. Section 3 introduces the manufacturing method of DES based on choline chloride, the thermophysical properties of prepared DES, and the experimental apparatus designed for this study. Section 4 shows experimental results and discussions on friction factor as a hydraulic characteristic and heat transfer coefficients as a thermal characteristic.

2. Theoretical Basis

2.1. Thermal Properties of Molten Salt, IL, and DES. The molten salt has been used as heat storage and a transfer medium in MSR, CSP, and ESS systems. It is very difficult to use molten salt for lab-scale experimental research due to its high operating temperature (>400°C) and corrosive properties [11]. In the case of ILs, it may be an alternative heat transfer medium of molten salt because it is a liquid at room temperature and ionized fluid such as molten salt. However, there are disadvantages in that expensive production cost, difficulty in synthesis, toxicity profiles, and lack of sustainability related to environmental and economic benefits [10, 12, 13]. Unlike molten salt and ILs, DESs are inexpensive, easy to synthesize, and nontoxic, so DESs have been recently employed as an alternative heat medium [6, 14]. However, since ILs and DESs do not have enough thermal applications, therefore, basic research on the thermal characteristics of these heat mediums is needed. As can be seen in Table 1, DESs have a lower melting point than molten salts. This means that ILs or DESs can be used as heat storage and transfer medium relatively easier than molten salts. So these can be applied to the thermal application in various ways; then these are expected to be applied to the energy industry in the near future.

2.2. Hydraulic and Thermal Boundary Layer of High Prandtl Number. The Prandtl number is a dimensionless number, defined as the ratio of momentum diffusivity to thermal diffusivity in heat transfer. The Prandtl number follows the following equation:

$$\mathrm{Pr} = \frac{\nu}{\alpha} = \frac{\text{Momentum diffusivity}}{\text{Thermal diffusivity}} = \frac{\mu/p}{k/C_p P} = \frac{C_p \mu}{k}, \quad (1)$$

where C_p is specific heat (J/kg·K), μ is viscosity (N·s/m^2), k is thermal conductivity (W/m·K), ρ is density (kg/m^3), and $C_p\rho$ is volumetric heat capacity (J/m^3·K). The Prandtl number is a physical variable that shows how much heat can transfer momentum and energy through diffusion and also represents the relationship between the hydraulic boundary and the thermal boundary layer. In general, water has the Prandtl number between 1 and 10, which means that the development of the hydraulic boundary layer is relatively faster than the thermal boundary layer as in Figure 1.

X shown in Figure 1 is the hydraulic boundary layer entrance length for the fluid, and X_T shown in Figure 1 is the thermal boundary layer entrance length. If the Prandtl number is lower than 1, Figure 1 shows that the hydraulic boundary layer developed after the thermal boundary layer is fully developed. However, if the Prandtl number is higher than 1, the thermal boundary layer developed after the flow boundary layer. Generally, DES Prandtl number is considerably high. Prandtl number for Glyceline, which is used in this study, is 248 at 80°C by calculation [10, 16]. It means that to observe the full development of the thermal boundary layer, a very long entrance length of the test section is required compared to the full development of the hydraulic boundary layer. Following on Prandtl number, the required length of test section is over the hundred meters. Therefore, to conduct a heat transfer characteristics study of a high Prandtl number fluid, an experimental loop should be designed in consideration of the thermal entrance length.

2.3. Existing Friction Factor and Nusselt Number Model/Correlations. This section introduces correlations between the friction factor and Nusselt number representing thermal-hydraulic characteristics of water. Usually, the friction factor measured through experiments is derived using the Darcy–Weisbach equation. In this equation, pressure drop (ΔP) and flow velocity (v) are measured, and other values are constant. Generally, this equation is used to calculate the friction factor. The experimental apparatus used in this experiment can get pressure data; also, the pipe radius and length of the test section are constant values. Therefore, the

Table 1: Melting Temperature, viscosity, and heat capacity of molten salt, ionic liquid, and DESs.

Fluid		Melting point (K)	Applications	Viscosity (mPa·s)	Heat capacity (J/K·kg)
Molten salt	LiF-NaF-KF (FLiNaK) @891K	727	Molten salt reactor thermal ESS high temperature concentrating solar power	0.0029	1,882.8
	LiF-BeF2 (FLiBe) @969K	733		0.0056	2,414.17
	KCl-MgCl2 @736K	708		0.0014	1,158.97
Ionic liquid	[C2MIm][BF4]	288.15	Dispersed hydrates aqueous two-phase (ATP) system absorption chiller	61.9 @298.15 K	1,556
	[C8MIm][BF4]	185.15		267 @298.15 K	1,765
	[C2MIm][EtSO4]	252.15		97.4 @298.15 K	1,620
DES	HBA HBD				
	ChCl Glycerol	327 (1:2)	Pretreatment of lignocellulosic date palm residues to enhance cellulose digestibility	259 @298.15 K	237.7 ± 0.6
	ChCl Urea	285 (1:2)		632 @298.15 K	180.05

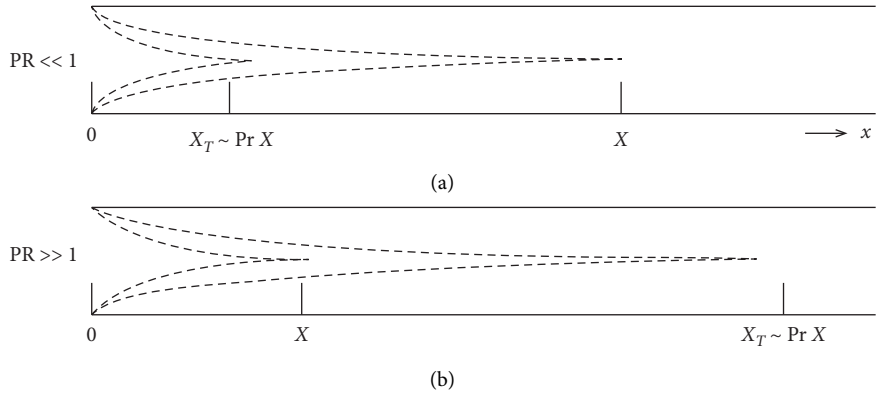

Figure 1: Prandtl number effect on the size of the hydrodynamic entrance length X relative to the size of the thermal entrance length X_T [15].

Darcy–Weisbach equation is a standard value for this experiment. This result value is compared using the Poiseuille equation in the laminar region and the Blasius correlation in the turbulent region. The Poiseuille formula is simple and most common to calculate friction factor in the laminar region [17]. The Blasius correlation is also the simplest numerical equation for calculating the friction factor in turbulent flow [17]. However, in the case of the Blasius correlation, it is only valid up to Reynolds number 20000. Therefore, the Filonenko correlation can be used over the 20000 Reynolds number. Blasius and Filonenko equations are used generally for calculating the friction factor of smooth circular pipes in turbulent flow [18]. Table 2 shows the detailed equations of the friction factor described above.

The Nusselt number is an important variable in convective heat transfer experiments. In the laminar region, the Shah–London correlation is often used for laminar flows [19]. In this experiment, the Chvetkov–Grigoryev correlation is also used to validate the accuracy and credibility of the experimental data because the temperature difference between the wall and the fluid may be largely due to the thermal boundary layer properties of the high Prandtl number fluid, and the resulting difference in viscosity is reflected [20]. In the turbulent region, the Dittus–Boelter equation is used, and in the case of Dittus–Boelter, it is a valid equation when the temperature difference between the wall and the fluid is small [21]. However, in this experiment, since the temperature difference is expected to be large, in addition to the Dittus–Boelter equation, Gnielinski and Sieder–Tate correlations are considered. In the case of the Gnielinski correlation, it is known to be effective in large Reynolds number range including transition region [21]. In addition, since the friction factor is included in the correlation, it is expected that the hydraulic properties of DES used in this experiment can be reflected. In the case of the Sieder–Tate correlation, it is known as a valid correlation when the temperature difference between the wall and the fluid is large. Moreover, since the Sieder–Tate correlation also includes the difference in viscosity according to the temperature of the wall and the fluid, such as the Chvetkov–Grigoryev correlation, it is expected to be suitable for DES, which is a high Prandtl number fluid. The convective

Table 2: Friction factor correlations in the single channel in laminar and turbulent regions.

Darcy–Weisbach	$f = 2(D/L)(1/\rho v^2)\Delta P$
Poiseuille	$f = 64/Re$
Blasius	$f = 0.3164Re^{-0.25}$ $(3{,}000 < Re \leq 2 \times 10^4)$
Filonenko	$f = (1.82\log\mathrm{Re} - 1.64)^{-2}$ $(\mathrm{Pr} = 0.6\sim10^5,\ 2300 < Re < 10^8)$

Table 3: Convective heat transfer correlations.

Shah–London (1978)	$Nu = 1.302((x/d)(1/\mathrm{RePr}))^{-(1/3)}$ $(\{(\mathrm{x/d})/(\mathrm{RePr})\} < 0.0001)$
Chvetkov–Grigoryev (2005)	$Nu = 4.36 + 1.31((1/\mathrm{RePr})(x/d))^{-(1/3)} \exp(-13\sqrt{(1/\mathrm{Re})(x/d)})(\mu_f/\mu_w)^{-1/6}$
Dittus–Boelter (1930)	$Nu = 0.023\mathrm{Re}_D^{0.8}\mathrm{Pr}^n$ $(0.6 < \mathrm{Pr} \leq 160,\ \mathrm{Re\ D} \geq 105,\ \mathrm{L/D} \geq 10,\ n = 0.4$ (for heating), $n = 0.3$ (for cooling))
Gnielinski (1983)	$Nu = (f/8)(\mathrm{Re}_D - 1000)\mathrm{Pr}/1 + 12.7(f/8)^{1/2}(pr^{2/3} - 1)$ $(0.5 < \mathrm{Pr} < 20{,}000,\ 3{,}000 < \mathrm{Re} < 5 \times 106)$
Sieder–Tate (1936)	$Nu = 1.86(\mathrm{RePr}(D/L))^{1/3}(\mu_f/\mu_w)^{0.14}$ (laminar) $Nu = 0.027\mathrm{Re}^{0.8}\mathrm{Pr}^{1/3}(\mu_f/\mu_w)^{0.14}$ (turbulent) $(0.7 < \mathrm{Pr} < 16{,}700,\ 104 < \mathrm{Re},\ \mathrm{L/D} > 60)$

heat transfer correlation and effective Reynolds number and Prandtl number ranges are summarized and shown in Table 3.

3. Experiments

This section will explain in detail the manufacture and verification of glyceline [16] as a heat transfer medium fluid and high Prandtl number fluid and also the design and verification of experimental apparatus to study the thermal-hydraulic characteristics of glyceline.

3.1. Manufacturing DES and Thermophysical Properties Analysis. In this study, glyceline was manufactured as a high Prandtl number heat transfer fluid. Glyceline is a DES synthesized with a molar ratio of 1:2 of choline chloride (CHCl, DAEJUNG, CAS No. 67-48-1) as a hydrogen bond acceptor (HBA) and glycerol (DAEJUNG, CAS No. 56-81-5) as a hydrogen bond donor (HBD). For reference, the formula and molar mass of CHCl are $C_5H_{14}ClNO$ and 139.62 g/mol, respectively, and the formula and molar mass of glycerol are $C_3H_8O_3$ and 92.094 g/mol, respectively. When putting those two substances in the large beaker, synthesis begins with a eutectic reaction. For fast and accurate synthesis, place the beaker on the hot plate stirrer and mix it for 2 hours under 70°C and 600 rpm conditions. To verify the DES is well synthesized, the density and viscosity were measured and compared with existing physical properties studies. In addition, the specific heat according to temperature increase was measured to study the heat transfer properties of manufactured DES.

In the case of density, it was calculated by measuring the volume change while increasing the DES temperature of a certain mass. The results of comparison with the result of the existing research [10] can be confirmed through Figure 2. In general, under steady pressure conditions, the density decreases when the temperature increases, and DES also shows the same trends. It was confirmed that the density value of the manufactured DES was measured within the 2.5% error range from the existing data. The viscosity of DES was also measured. The viscosity was measured using CAS's CL-L3

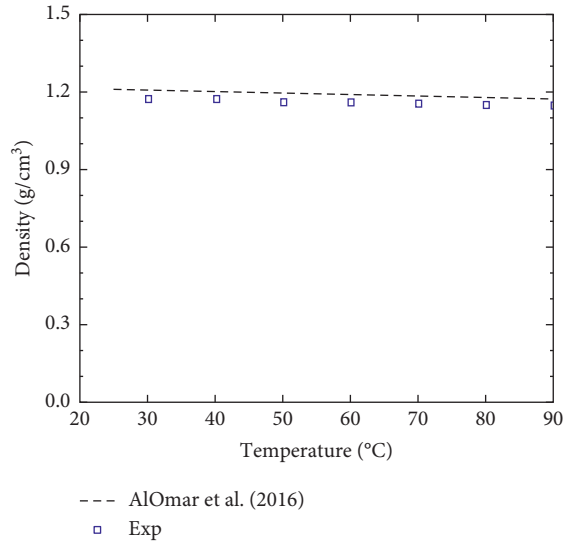

Figure 2: Density measurement of glyceline.

viscometer, and the viscosity error from the results of the previous study was within 1.06%. The viscosity measurement result is shown in Figure 3. Viscosity also decreases when the temperature increases. Specific heat is also an important property for heat transfer research, so DES from 20°C to 90°C was used to measure specific heat according to the temperature increase. As a result of measuring the specific heat, it showed that the specific heat increased as the temperature increased (Figure 4). It was confirmed that the DES was properly synthesized through density and viscosity data to perform the experiment, and the specific heat, which was not measured in the previous study, was measured to provide the foundation for the heat transfer characteristics of DES.

3.2. Experimental Test Loop

3.2.1. Experimental Apparatus. In order to study thermal-hydraulic characteristics of glyceline, friction factor and heat transfer coefficient need to be measured; for those

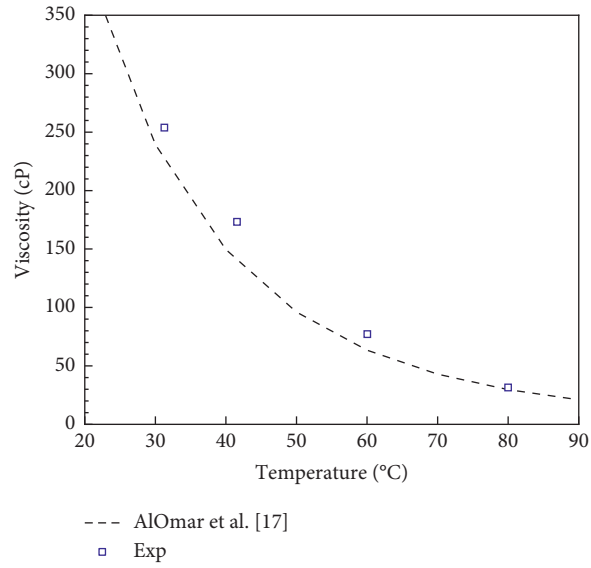

Figure 3: Viscosity measurement of glyceline.

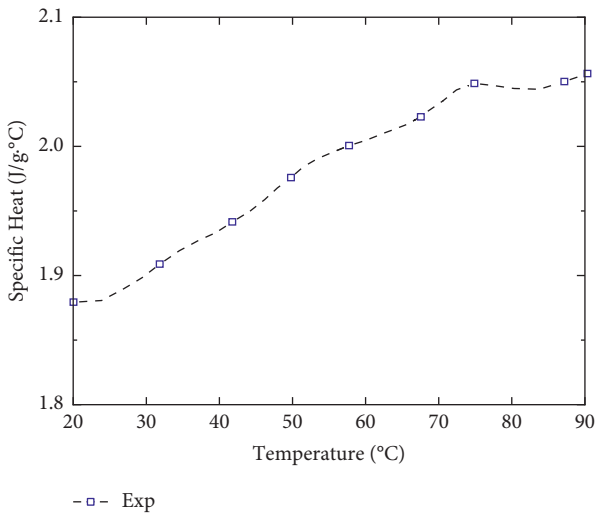

Figure 4: Specific heat measurement of glyceline.

properties, an experimental apparatus was designed. The important measurement value to quantify the friction factor is differential pressure in the test section. For measuring the heat transfer coefficient, the important measurement values are the temperature of the external wall of the test section and the temperature of the fluid at the inlet and the outlet of the test section. The design and construction of experimental apparatus that satisfy these major design requirements will be covered in this section.

The DES thermal-hydraulic characteristics experimental loop is shown in Figure 5. The reservoir for storing DES was designed to have a size of 300 mm in diameter and 260 mm in height to ensure a sufficient volume to fill the DES over the entire loop, and ceramic heaters were installed for heating and insulation. To control the temperature of the reservoir, heater power output was 400 mm controlled using test section inlet temperature and also installed chiller to prevent overheating of DES in the reservoir. Under the reservoir, a pump for transferring DES is placed. Two pumps are installed in parallel for each capacity to conduct experiments in various flow rate ranges and are designed to control the flow rates by adjusting the RPM of the pumps. Flow meters were installed downstream of the pumps, and flow meters corresponding to the discharge flow rate change of each pump were installed to measure the discharge flow rate. A flow control valve was connected downstream of the flow meter to adjust the flow rate discharged from the pumps to control a smaller flow rate, and a pump bypass to the flow path was made at the front of the flow control valve to protect the pumps. The DES went through the flow meter to pass through the two elbow curves, and at this time, the flow velocity profile is deformed. To get hydraulic fully developed flow, the entrance length of the pipe flow is calculated by equation (2) [22]. Following equation (2), the entrance length for the maximum Reynolds number 3000 in this experiment is 109.83 mm. Therefore, an entrance length of 400 mm was secured so that the fluid could be hydraulic fully developed before going into the test section.

$$L_{\text{turbulent}} = 1.359\ D(\text{Re})^{1/4}. \quad (2)$$

The test section is basically designed horizontally to prevent static pressure changes due to height differences. A more detailed description of the test section will be given in the next section. The heated DES discharged from the test section is circulated to the reservoir and then forms a circulation loop again.

To verify the validation of flow meters and differential pressure sensors, the difference between the measured and calculated data using water was compared. As shown below in Figures 6 and 7, the error between the measured and calculated data was less than 3%; therefore, the validation of the flow meters and differential pressure sensors were proven.

For the thermocouple, it has proved compared with measured value through thermal imaging camera, and the error was estimated under 4%. The thermal imaging camera used in this experiment is testo 890; its sensitivity to heat is under 40 mK at 30°C. And the temperature measurement range of this camera is from −30°C to 100°C with ±2% of accuracy.

3.2.2. Test Section. As shown in Figure 8, the test section is a circular tube of stainless steel (SUS 316) with a length of 920 mm, an inner diameter of 10.92 mm, and a thickness of 0.89 mm. Test section in a part heated by DC power supply after passing an entrance length of 400 mm. Nichrome wires were used as heat sources for heating the test section. The nichrome wires used have a diameter of 1.25 mm with a resistance of 6 Ω/m and is tightly wrapped around the outer wall of the test section to give a uniform heat flux throughout the test section. The total length of the heating wire to wrap the outer wall of the test section is 11,920 mm. In order to connect the heating wire surrounding the test section to the DC power supply, two wires were connected by soldering

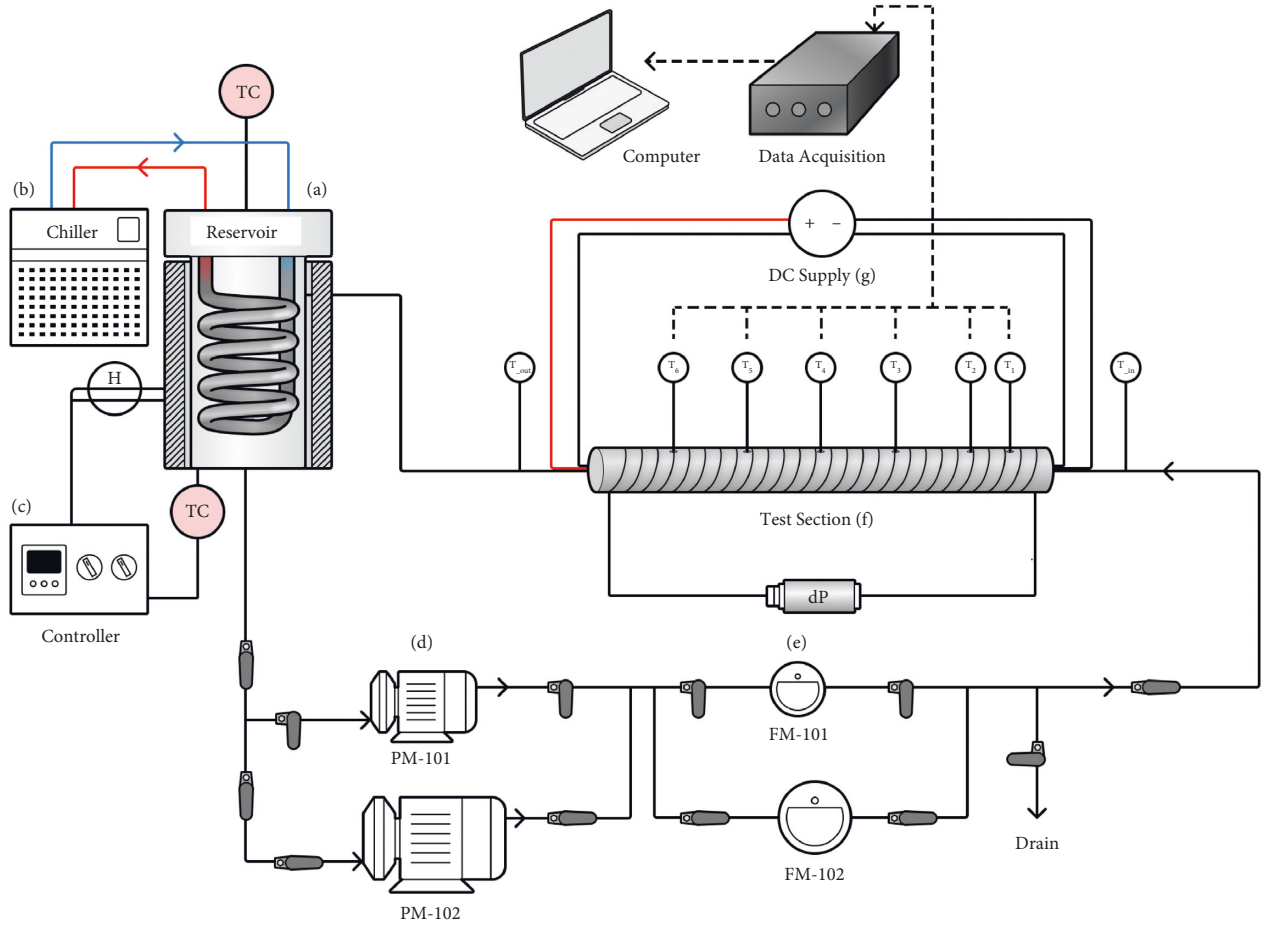

Figure 5: Experimental test loop: (a) thermal reservoir, (b) chiller, (c) DES temperature controller, (d) pump, (e) flow meter, (f) test section, and (g) DC power supply.

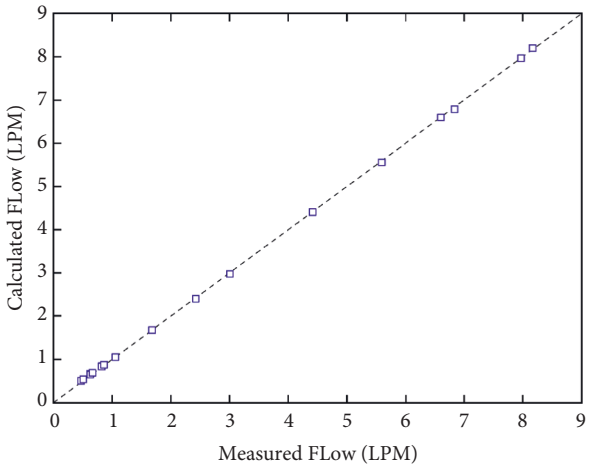

Figure 6: Validation experiment of flow meters.

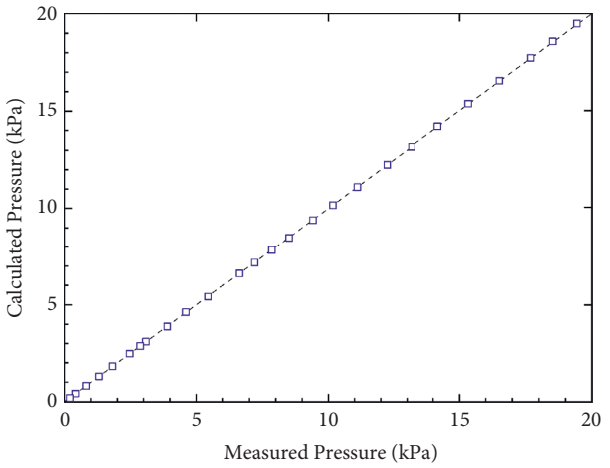

Figure 7: Validation experiment of differential pressure sensors.

between those three wires. This process is to prevent heat loss through the connection part when the heating wire is directly connected to the DC power supply. Also, when using a DC power supply, the remote control method is used to measure the voltage and current applied to the heating wire more accurately. In order to minimize the heat loss to the outside of the test section, a thermal insulator (glass wool) is used and insulated to a thickness of 100 mm. A differential pressure line is connected at both ends of the test section to measure pressure difference. Valves are installed up/downstream of the differential pressure transmitter to remove air bubbles present in that line.

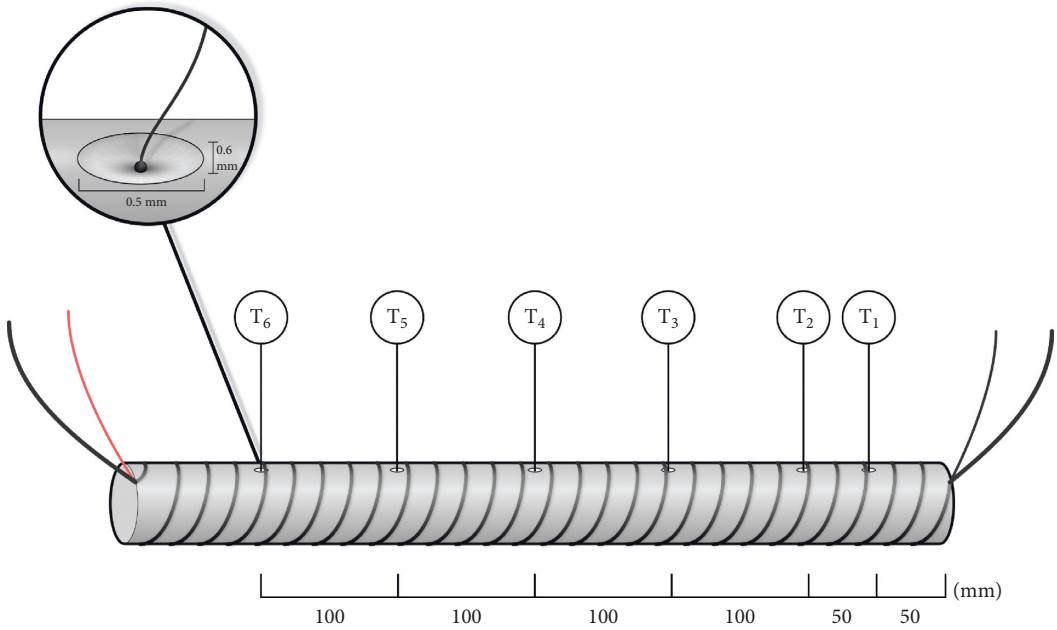

Figure 8: Details of test section design with TC installation detail.

The temperature data required to measure the heat transfer coefficient are the wall temperature of the test section and the inlet/outlet temperature of the fluid. The inlet/outlet temperature of the fluid is measured using *K*-type thermocouples, and the surface wall temperature of the test section is measured also using a total of six *K*-type thermocouples, starting with the inlet, two at intervals of 50 mm and then the last four at intervals of 100 mm. For accurate measurement of the temperature of the surface wall of the test section, a hole with a depth of 0.6 mm and a diameter of 0.5 mm was dug into the surface shown in Figure 8, and thermocouples are fixed to each hole using a silver paste.

3.3. Validation Test of Experimental Apparatus. In order to verify the performance of the fabricated experimental apparatus, a friction factor measurement test was carried out using water. In the case of water, due to its theoretical formula explaining the friction factor in the laminar and turbulent region, the validation test of this apparatus was performed by confirming whether the measured friction factor coincides with the theoretical values. Figure 9 shows the result of the experimental apparatus validation test. As a result of the test, it was confirmed that when the Reynolds number was under 3000, the friction factor values were consistent with the Poiseuille equation, which is the theoretical value in the laminar region. Reynolds number between 3000 and 7000 is the transition region, and that over 7000 is the turbulence region, and it can be verified through the measured friction factor and the Blasius equation are consistent, which is theoretical value in turbulence.

In addition to verifying the validity of the experimental apparatus, a heat transfer coefficient measurement test was carried out using water, and the result is shown in Figure 10.

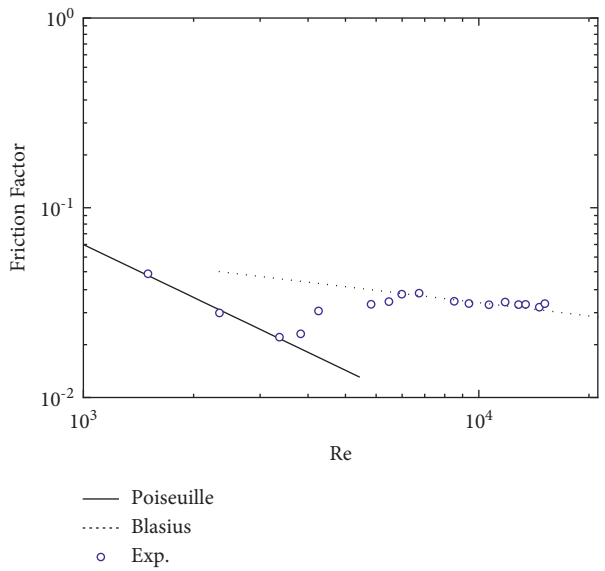

Figure 9: Measured friction factor results using water.

The experimental results were compared with the Chvetkov–Grigoryev correlation, and the error between the correlation and experimental value was within 10.53%. Through a verification experiment using water, it shows that this apparatus is valid to perform thermal-hydraulic experiments.

4. Results and Discussion

4.1. Measurement Results of glyceline Friction Factor. The experiment was performed under the condition shown in Table 4 to measure the friction factor of DES. To conduct the friction factor measurement experiment within various

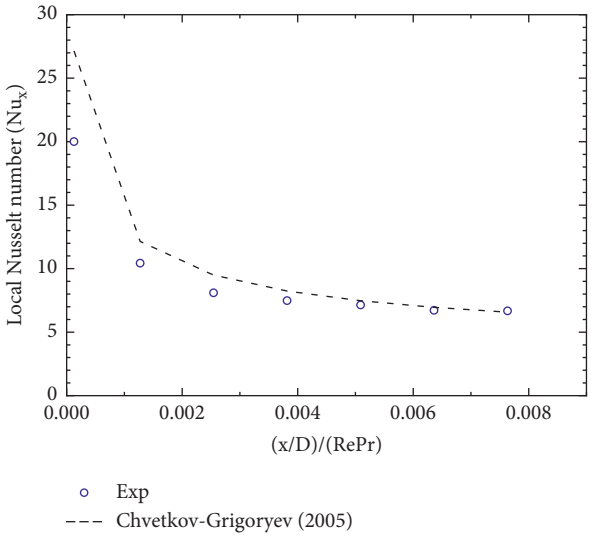

Figure 10: Measured Nusselt number results using water.

Table 4: Experimental conditions for measurement of friction factor.

Temp.(°C)	Re	Density (kg/m^3)	Viscosity (Pa·sec)
50°C	166~232	1,195.225	0.0961
80°C	440~1703	1,180.225	0.0297
100°C	831~3063	1,170.225	0.0151

Reynolds number ranges, the experiment was carried out while maintaining the temperatures of DES constant of 50°C, 80°C, and 100°C. In addition, differential pressure and friction factor were measured by controlling the flow rate of the pump under a constant temperature. The friction factor was calculated using the Darcy–Weisbach equation in Table 2. Figure 11 shows the measurement results of the friction factor according to the change in the Reynolds number.

As a result of measuring the friction factor, glyceline is a Newtonian fluid, and it follows the existing theoretical equation. In the laminar flow region, the measured value of the friction factor of glyceline had an error up to 15% with the Poiseuille equation, and in the turbulent region, a maximum error of 12% occurred between the Blasius equation and experimental value. Friction factor results of water case shown in Figure 9, the transition region comes after 3000 Reynolds number; on the contrary, Figure 11 identifies that transition region for glyceline from laminar region to turbulent region occurs near 1200 Reynolds number, and this is the difference from the existing fluid discovered through this study.

4.2. Measurement Results of Glyceline Heat Transfer Coefficient

4.2.1. Thermal Loss Analysis. Thermal loss was quantified to ensure the validity of the results of this experiment, and the results will be shown in this section. To calculate thermal loss, the following equation shown below is used:

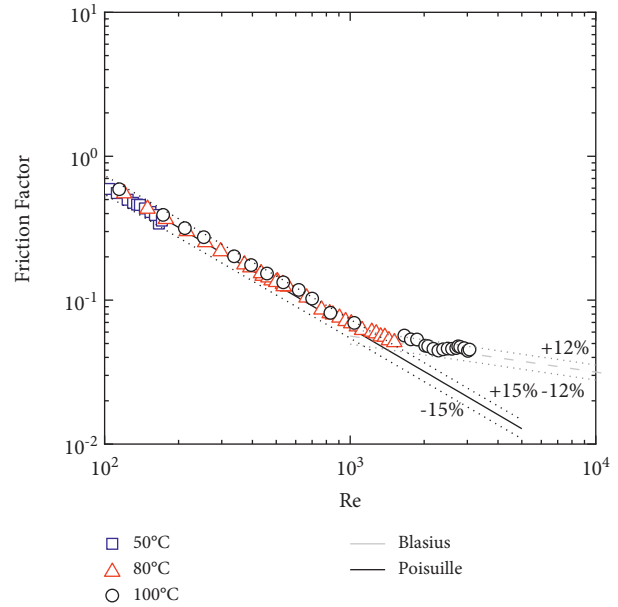

Figure 11: Measurement results of friction factor of glyceline.

$$Q_{\text{loss}} = \frac{2\pi kL(T_2 - T_1)}{\ln(r_2/r_1)}. \tag{3}$$

In the experiment, KCC's Cerakwool 1300 Blanket product was used for glass wool as an insulator. k is the thermal conductivity of glass wool covering the outside of the test section ($k = 0.03$), and L is the length of the pipe at the test section ($L = 0.6$ m). T_1 is the temperature outside the test section, which is the room temperature (25°C); T_2 is the temperature of the heater ($T_{htr.Max} = 127.2$°C); r_1 is the pipe radius ($r_1 = 5.46$ mm); and r_2 is the distance (radius) from the center of the test section ($r_1 = 50$ mm) to the heat insulating unit. The thermal loss calculated through the above equation was 4.4%, which shows the insulating of this experimental apparatus is well designed.

4.2.2. Measurement Results of Heat Transfer Coefficient. After measuring the heat loss, the heat transfer coefficient measurement experiment is carried out. Figure 12 illustrates the results of the heat transfer coefficient experiment conducted through this research, and it shows the local Nusselt number depending on the change in the Reynolds number. Nusselt number calculation is shown equation (4). In each graph, the X-axis represents a dimensionless distance; the left-to-right direction represents the exit direction from the inlet; and the Y-axis represents the local Nusselt number. Since glyceline is a high Prandtl fluid, it cannot be thermally fully developed in this experimental apparatus.

Nusselt number calculation is as follows:

$$Nu = \frac{hD}{k},$$

$$h = \frac{q}{A \times \Delta T}, \tag{4}$$

$$\Delta T = T_{\text{wall}} - T_{\text{fluid}}.$$

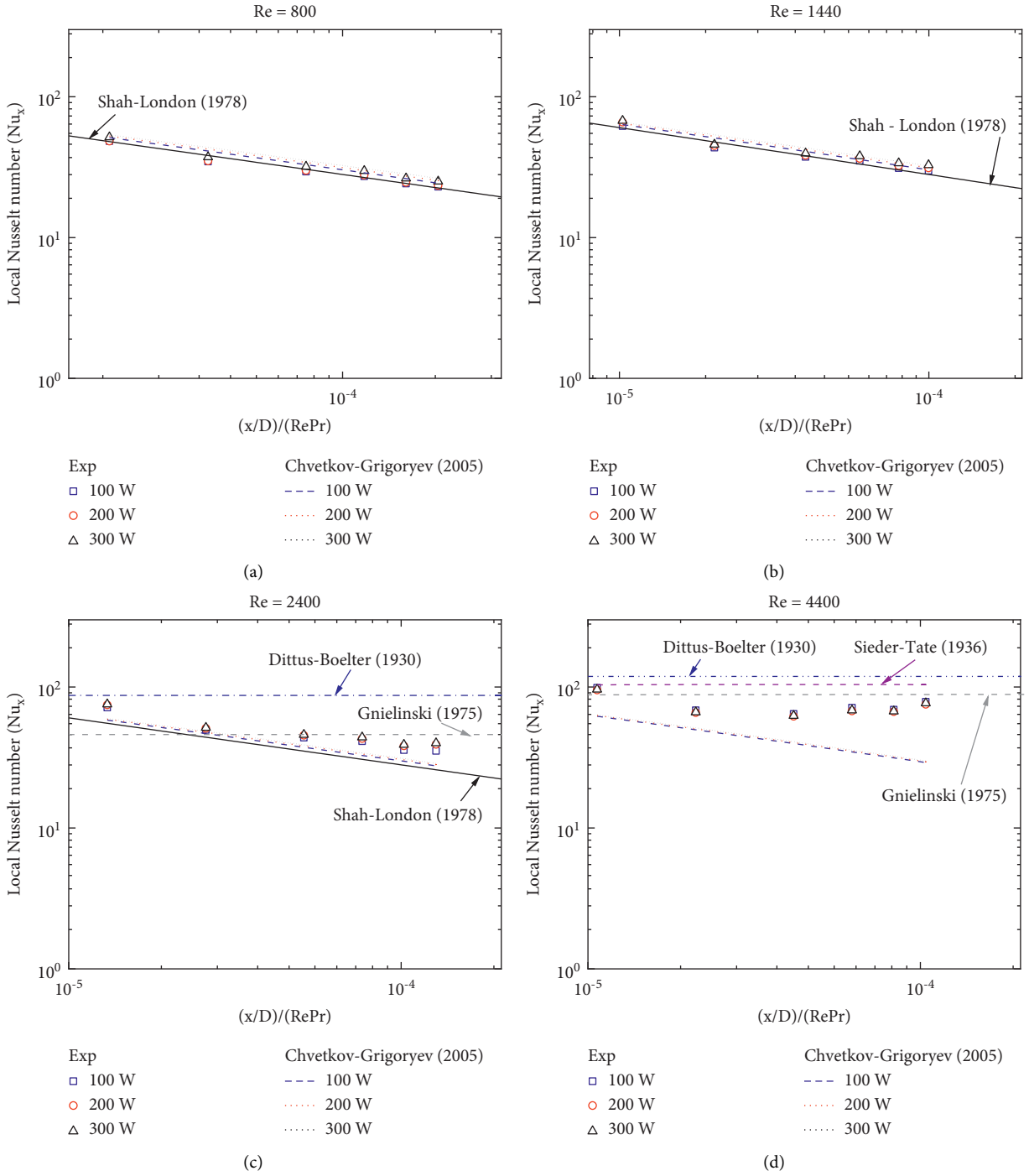

Figure 12: Nusselt number of glyceline: (a) Re = 800, (b) Re = 1440, (c) Re = 2400, and (d) Re = 4400.

Therefore, it is not possible to directly compare based on the definition of the Nusselt number ($Nu = hd/k$); it is compared with the two correlations, Shah–London [20] and Chvetkov-Grigoryev [23], according to the change of dimensionless distance in the laminar region. Reproducibility is also confirmed by performing an experiment by changing the output power to 100 W, 200 W, and 300 W through a DC power supply for each Reynolds number.

Figure 12(a) is the result of the heat transfer coefficient at Reynold number 800. As it goes toward the outlet, the local Nusselt number decreases to the log scale. Since this experimental condition is in the laminar region, it is well matched with the Shah–London correlation, which is the Nusselt correlation in the laminar region. In addition, since the results are almost the same according to the change in output, it can be determined that the reproducibility of this

experiment is also guaranteed. As the friction factor of glyceline in the laminar region is well agreed with the theory, it can be confirmed that the heat transfer coefficient properties in the laminar region are also well matched with the existing theory. The root mean square error (RMSE) between experimental results and the Shah–London correlation value is 2.2%. In addition, it is compared with the Chvetkov–Grigoryev correlation, which includes differences in viscosity between wall and fluid that can reflect the heat transfer coefficient properties of high Prandtl fluids. The RMSE between experimental values and the Chvetkov–Grigoryev correlation value is 5.36%. Chvetkov–Grigoryev correlation predicts the Nusselt number 3.14% higher than the Shah–London correlation, which is decided to be the difference between the viscosity on the wall, and it is on the fluid in the Chvetkov–Grigoryev correlation. Through this experiment, the difference in viscosity due to the temperature difference between the wall and the fluid is not significant even if the thermal boundary layer of the high Prandtl number fluid is not fully developed.

Figure 12(b) is the result of the heat transfer coefficient at Reynold number 1440. In the results of the friction factor experiment, it shows that a transition region occurs around the Reynolds number is around 1200. However, the result of the heat transfer coefficient experiment confirms that even when Reynolds number is 1440, it is consistent with the Nusselt number correlation in the laminar region. The RMSE between the Shah–London correlation, which is the correlation in the laminar region, and the experimental result is 3.4%, and RMSE with the Chvetkov–Grigoryev is calculated as 4.8%. It is determined that the reason why the Reynolds number entering the transition region is different in the friction factor experiment and the heat transfer coefficient experiment is that the hydraulic developed length and the thermal developed length are different. In other words, as glyceline is a high Prandtl fluid; the thermal boundary layer develops later as shown in Figure 1.

Figure 12(c) is the result of the heat transfer coefficient at Reynold number 2400. As a result of the experiment, the local Nusselt number shifts from the laminar region correlations to the turbulent region correlations as increases in Reynolds number. It means that the transition Reynolds number in heat transfer is much higher than the one in friction factor. The RMSE between the Shah–London correlation, which is the correlation in the laminar region, and the experimental result is 12.51%, and RMSE with the Chvetkov–Grigoryev is 9.85%. On the other hand, the RMSE with the turbulent region correlation Dittus–Boelter is 39.87%, and the RMSE between Gnielinski correlations is 16.7% as calculated. In the case of the Dittus–Boelter equation, it more accurately predicts the Nusselt number when there is a little temperature difference between the bulk fluid and the wall. However, glyceline used in this experiment is a high Prandtl number fluid, so the differential temperature between the bulk fluid and the wall is large, resulting in a large error with the Dittus–Boelter equation is occurred.

Figure 12(d) is the result of the heat transfer coefficient at Reynold number 4400. As a result of the experiment, the local Nusselt number moved from the laminar region to the turbulent region when the Reynolds number is 2400. The RMSE with the turbulent region correlation Dittus–Boelter is 44.3%; that between Gnielinski correlations is 15.6%; and that between Sieder–Tate correlations is 28.8% as calculated. As discussed above, it is judged that the Dittus–Boelter equation is not suitable for application to high Prandtl fluid. Since the Sieder–Tate correlation is a valid correlation with a Reynolds number of 10000 or more, which is not included in this experiment's Reynolds number range; therefore, it is estimated that the error with the experimental data is large. In summary, the heat transfer coefficient properties of glyceline are predictable by the Shah–London and Chvetkov–Grigoryev correlation in the laminar region and by the Gnielinski correlation in the turbulent region. However, since glyceline is a high Prandtl number fluid, the thermal boundary layer develops slower than the hydraulic boundary layer, so it was confirmed that there is a difference between the transition region identified through the friction factor, and it is through the heat transfer coefficient experiment.

5. Conclusion

This research conducted thermal-hydraulic experiments using glyceline, a type of transparent salt with low melting point and visibility as a fundamental study of molten salt used as a heat transfer and storage medium in an MSR and concentrate solar power (CSP). An experimental apparatus was designed and constructed for this research, and the validation of this apparatus was verified using water.

Through this study, the friction factor and heat transfer coefficient of glyceline were measured. As a result of the experiment, it is confirmed that glyceline is a Newtonian fluid, and data are well matched with the Poiseuille equation and the Blasius correlation in laminar and turbulent flow regions, respectively. And an error in two flow regions is within 15% and 12% compared to the existing theoretical equations. The difference from water appears in the transition area. The transition region for water appears when the Reynolds number is 2300, while it for glyceline appears when the Reynolds number is 1200. This result means that the transition region could change depending on the composition of the molten salt, which means that empirical verification is required in studying the thermal-hydraulic characteristics of the molten salt.

In the case of the heat transfer coefficient experiment, since glyceline is a high Prandtl number fluid, the local Nusselt number according to dimensionless length is compared to and analyzed with the existing theoretical equations. Overall, it confirms that the local Nusselt number shifts from the laminar region to the turbulent region as the Reynolds number increases, but the thermal transition region appears with a larger Reynolds number than the hydraulic transition region. In the laminar region (Re = 800), it is compared with the Shah–London and Chvetkov–Grigoryev correlations, and it is confirmed that the experimental data is consistent with the error range of up to 2.2% and 5.36%, respectively. In the turbulent region (Re = 4400), it is compared with the Dittus–Boelter equation and

Gnielinski correlations, and it is confirmed that the experimental data is consistent with the error range of up to 44.3% and 15.6%, respectively. However, it is confirmed that the transition region occurred at around when Reynolds number is 2400, unlike in friction factor, due to the characteristics of high Prandtl number fluid in which the thermal boundary layer develops later than the hydraulic boundary layer.

In conclusion, the thermal-hydraulic characteristics of DES can be explained through existing equations and correlations. However, it is confirmed experimentally that hydraulic and thermally transition from laminar to turbulent have a large difference. Therefore, it is judged that a thermal-hydraulic experiment for every system using high Pr liquid including molten salt and DES is necessary for effective usage as thermal storage and transfer mediums.

Nomenclature

T_{wall}: Wall temperature (K)
T_{fluid}: Fluid temperature (K)
v: Velocity (m/sec)
ΔP: Pressure difference (Pa)
ρ: Density (Kg/m^3)
D: Hydraulic diameter (m)
L: Test section length (m)
A: Heat area (m^2)
f: Friction factor (dimensionless)
k: Thermal conductivity (W/m·K)
h: Heat transfer coefficient (W/m^2·K)
μ_f: Fluid viscosity center of pipe (Pa·sec)
μ_w: Fluid viscosity near wall (Pa·sec)
Re: Reynolds number (dimensionless)
Nu: Nusselt number (dimensionless)
Pr: Prandtl number (dimensionless).

Data Availability

The data used to support this study are available at https://doi.org/10.6084/m9.figshare.19221960.v1.

Conflicts of Interest

The authors declare that they have no conflicts of interest.

Acknowledgments

This work was supported by the National Research Foundation of Korea (NRF) grant funded by the Korean government (MSIP; Nos. 2017M2A8A4018624 and 2017M2A8A4018812) and supported by Korea Hydro & Nuclear Power Co. (2021).

References

[1] Q. Li, Y. Liu, S. Guo, and H. Zhou, "Solar energy storage in the rechargeable batteries," *Nano Today*, vol. 16, pp. 46–60, 2017.

[2] C. S. Singer, S. Giuliano, and R. Buck, "Assessment of improved molten salt solar tower plants," *Energy Procedia*, vol. 49, pp. 1553–1562, 2014.

[3] M. A. Miller, J. Petrasch, K. Randhir, N. Rahmatian, and J. Klausner, "Chemical energy storage," in *Thermal, Mechanical, and Hybrid Chemical Energy Storage Systems*, pp. 249–292, Academic Press, Cambridge, UK, 2021.

[4] N. Breidenbach, C. Martin, H. Jockenhöfer, and T. Bauer, "Thermal energy storage in molten salts: overview of novel concepts and the DLR test facility TESIS," *Energy Procedia*, vol. 99, pp. 120–129, 2016.

[5] S. B. Seo, "Study on heat transfer behavior of high-prandtl number fluid and its feasibility to passive heat transport system," 2018, https://scholarworks.unist.ac.kr/handle/201301/24653.

[6] A. P. Abbott, D. Boothby, G. Capper, D. L. Davies, and R. K. Rasheed, "Deep eutectic solvents formed between choline chloride and carboxylic acids: versatile alternatives to ionic liquids," *Journal of the American Chemical Society*, vol. 126, pp. 9142–9147, 2004.

[7] M. Hayyan, F. S. Mjalli, M. A. Hashim, and I. M. AlNashef, "A novel technique for separating glycerine from palm oil-based biodiesel using ionic liquids," *Fuel Processing Technology*, vol. 91, pp. 116–120, 2010.

[8] V. Migliorati, F. Sessa, and P. D'Angelo, "Deep eutectic solvents: a structural point of view on the role of the cation," *Chemical Physics Letters*, vol. 737, Article ID 100001, 2019.

[9] E. L. Smith, A. P. Abbott, and K. S. Ryder, "Deep eutectic solvents (DESs) and their applications," *Chemical Reviews*, vol. 114, no. 21, pp. 11060–11082, 2014.

[10] M. K. AlOmar, M. Hayyan, M. A. Alsaadi, S. Akib, A. Hayyan, and M. A. Hashim, "Glycerol-based deep eutectic solvents: physical properties," *Journal of Molecular Liquids*, vol. 215, pp. 98–103, 2016.

[11] D. Kearney, U. Herrmann, P. Nava et al., "Assessment of a molten salt heat transfer fluid in a parabolic trough solar field," *Journal of Solar Energy Engineering*, vol. 125, no. 2, pp. 170–176, 2003.

[12] B. Wu, R. G. Reddy, and R. D. Rogers, "Novel ionic liquid thermal storage for solar thermal electric power systems," in *Proceedings of the International Solar Energy Conference*, Washington, DC, USA, 2001.

[13] L. Moens, D. M. Blake, D. L. Rudnicki, and M. J. Hale, "Advanced thermal storage fluids for solar parabolic trough systems," *Journal of Solar Energy Engineering*, vol. 125, no. 1, pp. 112–116, 2003.

[14] V. Fischer, *Properties And Applications of Deep Eutectic Solvents and Low-Melting Mixtures*, Doctoral Dissertation, der Universität Regensburg, Regensburg, Germany, 2015.

[15] A. Bejan, *Convection Heat Transfer*, John wiley & sons, Hoboken, NJ, USA, 2013.

[16] A. Singh, R. Walvekar, M. Khalid, W. Y. Wong, and T. C. S. M. Gupta, "Thermophysical properties of glycerol and polyethylene glycol (PEG 600) based DES," *Journal of Molecular Liquids*, vol. 252, pp. 439–444, 2018.

[17] K. M. Assefa and D. R. Kaushal, "A comparative study of friction factor correlations for high concentrate slurry flow in smooth pipes," *Journal of Hydrology and Hydromechanics*, vol. 63, no. 1, pp. 13–20, 2015.

[18] X. Fang, Y. Xu, and Z. Zhou, "New correlations of single-phase friction factor for turbulent pipe flow and evaluation of existing single-phase friction factor correlations," *Nuclear Engineering and Design*, vol. 241, no. 3, pp. 897–902, 2011.

[19] B. Kristiawan, B. Santoso, W. E. Juwana, R. M. Ramadhan, and I. Riandana, "Numerical investigation of laminar convective heat transfer for TiO2/water nanofluids using two-

phase mixture model (Eulerian approach)," *AIP Conference Proceedings*, vol. 1788, 2017.

[20] R. K. Shah and A. L. London, *Laminar Flow Forced Convection in Ducts: A Source Book for Compact Heat Exchanger Analytical Data*, Academic press, Cambridge, UK, 2014.

[21] *Dittus-Boelter Equation: Correlation & Calculation. Nuclear Power*, 2022, https://www.nuclear-power.com/nuclear-engineering/heat-transfer/convection-convective-heat-transfer/dittus-boelter-equation/.

[22] Y. A. Çengel, *Fluid Mechanics: Fundamentals and Applications*, mcgraw-hill education, New York, NY, USA, 2018.

[23] F. F. Chvetkov and B. A. Grigoryev, *Heat-Mass Exchange*, p. 550, Moscow Power Engineering Institute Publishing, Moscow, 2005.